Acta Crystallographica Section A
Foundations of Crystallography
ISSN 0108-7673

Received 12 February 2001
Accepted 9 May 2001

Theoretical investigation of metastable Al_2SiO_5 polymorphs

Artem R. Oganov,* G. David Price and John P. Brodholt

Crystallography and Mineral Physics Unit, Department of Geological Sciences, University College London, Gower Street, London WC1E 6BT, England. Correspondence e-mail: a.oganov@ucl.ac.uk

Using theoretical simulations based on density functional theory within the generalized gradient approximation, a series of metastable phase transitions occurring in low-pressure Al_2SiO_5 polymorphs (andalusite and sillimanite) are predicted; similar results were obtained using semiclassical interatomic potentials within the ionic shell model. Soft lattice modes as well as related structural changes are analysed. For sillimanite, an isosymmetric phase transition at *ca* 35 GPa is predicted; an incommensurately modulated form of sillimanite can also be obtained at low temperatures and high pressures. The high-pressure isosymmetric phase contains five-coordinate Si and Al atoms. The origin of the fivefold coordination is discussed in detail. Andalusite was found to transform directly into an amorphous phase at *ca* 50 GPa. This study provides an insight into the nature of metastable modifications of crystal structures and the ways in which they are formed. Present results indicate the existence of a critical bonding distance, above which interatomic interactions cannot be considered as bonding. The critical distance for the Si—O bond is 2.25 Å.

1. Introduction

Metastability phenomena play an important role in many natural and technological processes. For instance, according to the famous Ostwald's rule, crystallization often produces a metastable phase, which slowly transforms into the stable modification *via* a sequence of metastable phases. At low temperatures, because of kinetics, metastable phases can exist indefinitely long. Amorphous solids are just one example of this metastability. Recent discoveries, *e.g.* of pressure-induced amorphization by Mishima *et al.* (1984) and the 'memory glass effect' by Kruger & Jeanloz (1990),[1] have boosted interest in metastability phenomena. It is possible, for instance, that ice comets consist, to a large extent, of amorphous ice phases, formed at high pressure and low temperatures. Another example is provided by isosymmetric phase transitions, which can lead to both stable [*e.g.* $KTiOPO_4$ (see Alan & Nelmes, 1996)] and metastable [*e.g.* SiO_2 (Badro *et al.*, 1997)] phases. This type of phase transitions, until recently thought to be very unusual, is now being found in an increasing number of systems.

Theoretically, for any compound there can be an infinite number of metastable structures, corresponding to local minima of the free-energy hypersurface.[2] However, only a small number of these possibilities can practically be synthesized. Theoretical simulations can often shed light on the nature of such phases (Tse & Klug, 1992) and can even be used to predict their behaviour and optimal conditions for their synthesis. Here we report state-of-the-art theoretical simulations of metastable phases in the Al_2SiO_5 system. The variety of metastable phases predicted here make Al_2SiO_5 an ideal subject for studies of metastability phenomena.

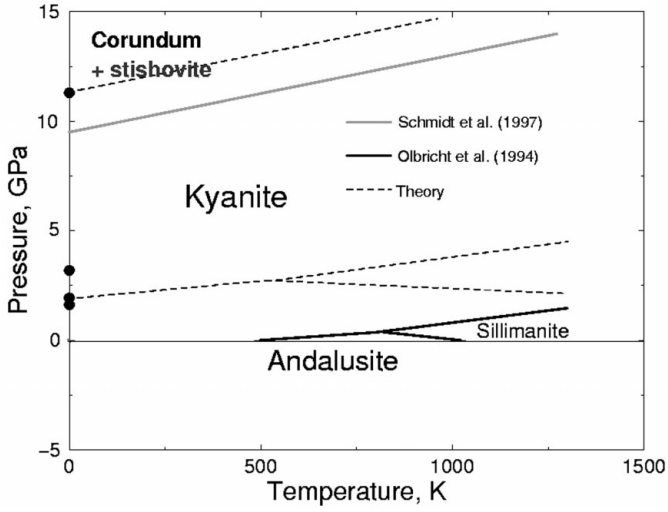

Figure 1
Phase diagram of Al_2SiO_5. Theoretical results are from Oganov & Brodholt (2000). Experimental results are from Olbricht *et al.* (1994) and Schmidt *et al.* (1997). At high pressures, the mixture of oxides (corundum Al_2O_3 and stishovite SiO_2) is more stable than any of the Al_2SiO_5 polymorphs. As metastable phases, however, all these polymorphs can exist at pressures well above their regions of thermodynamic stability.

[1] It is becoming increasingly evident that the 'memory glass effect' was an experimental artifact.
[2] Metastable phases do not transform to the stable phases at low temperatures because it takes some energy to overcome the activation barrier and displace the system from a local minimum. At high temperatures, such energy is available and transitions to the stable phase become kinetically feasible.

Table 1
Comparison of theoretical calculations with experimental data for sillimanite.

The experimental crystal structure was taken from Winter & Ghose (1979), the equation of state was taken from Yang *et al.* (1997), and the atomization energy was recalculated from the enthalpy of formation data of Olbricht *et al.* (1994). [4] means that fixed $K' = 4$ was assumed in fitting the equation of state.

	GULP	*VASP*	Experiment
Unit-cell parameters and volume			
a_0 (Å)	7.151	7.555	7.4883
b_0 (Å)	7.540	7.756	7.6808
c_0 (Å)	5.918	5.795	5.7774
V_0 (Å^3)	319.11	339.57	332.29
Atomic coordinates (space group *Pbnm*)			
Al1	(0, 0, 0)	(0, 0, 0)	(0, 0, 0)
Al2	(0.1374, 0.3420, 1/4)	(0.1429, 0.3464, 1/4)	(0.1417, 0.3449, 1/4)
Si	(0.1512, 0.3359, 3/4)	(0.1530, 0.3413, 3/4)	(0.1533, 0.3402, 3/4)
O_a	(0.3702, 0.4022, 3/4)	(0.3594, 0.4110, 3/4)	(0.3605, 0.4094, 3/4)
O_b	(0.3572, 0.4360, 1/4)	(0.3571, 0.4342, 1/4)	(0.3569, 0.4341, 1/4)
O_c	(0.4744, 0.0036, 3/4)	(0.4776, 0.0020, 3/4)	(0.4763, 0.0015, 3/4)
O_d	(0.1232, 0.2230, 0.5120)	(0.1253, 0.2239, 0.5135)	(0.1252, 0.2230, 0.5145)
Physical properties			
E_{atom} (eV)	–	−50.795	−51.19
K_0 (GPa)	161.4 (155.9 with $K' = 4$)	160.1 (148.0 with $K' = 4$)	171
K'	2.99	2.69	[4]

Table 2
Comparison of theoretical calculations with experimental data for andalusite.

The experimental crystal structure was taken from Winter & Ghose (1979), the equation of state was taken from Ralph *et al.* (1984) and included a later correction by Yang *et al.* (1997), and the atomization energy was recalculated from the enthalpy of formation data of Olbricht *et al.* (1994).

	GULP	*VASP*	Experiment
Unit-cell parameters and volume			
a_0 (Å)	7.679	7.860	7.7980
b_0 (Å)	7.727	7.956	7.9031
c_0 (Å)	5.666	5.592	5.5566
V_0 (Å^3)	336.21	349.68	342.45
Atomic coordinates (space group *Pnnm*)			
Al1	(0, 0, 0.2472)	(0, 0, 0.2419)	(0, 0, 0.2419)
Al2	(0.3605, 0.1395, 1/2)	(0.3709, 0.1389, 1/2)	(0.3705, 0.1391, 1/2)
Si	(0.2304, 0.2550, 0)	(0.2458, 0.2522, 0)	(0.2460, 0.2520, 0)
O_a	(0.4555, 0.3511, 1/2)	(0.4243, 0.3627, 1/2)	(0.4233, 0.3629, 1/2)
O_b	(0.4120, 0.3714, 0)	(0.4238, 0.3640, 0)	(0.4246, 0.3629, 0)
O_c	(0.0941, 0.4106, 0)	(0.1025, 0.4006, 0)	(0.1030, 0.4003, 0)
O_d	(0.2262, 0.1451, 0.2305)	(0.2311, 0.1341, 0.2401)	(0.2305, 0.1339, 0.2394)
Physical properties			
E_{atom} (eV)	–	−50.844	−51.23
K_0 (GPa)	208.9 (196.2 with $K' = 4$)	145.3 (143.5 with $K' = 4$)	135; 151
K'	1.83	3.88	[4]; [4]

The Al_2SiO_5 polymorphs (kyanite, andalusite and sillimanite) are well known in mineralogy (Kerrick, 1990). For a long time, their geologically important phase diagram was a matter of debate, which now seems to have been resolved (Olbricht *et al.*, 1994). The main source of the problems in the experimental determination of this phase diagram was the small energy differences between the polymorphs and the resulting kinetic problems. In our previous work (Oganov & Brodholt, 2000), we reproduced the experimental phase diagram rather closely (Fig. 1) using state-of-the-art quantum-mechanical simulations; the electronic structure of these minerals was recently studied (Iglesias *et al.*, 2001) using a similar method. At pressures above 11 GPa, Al_2SiO_5 phases become thermodynamically unstable and decompose into a mixture of oxides, Al_2O_3 plus SiO_2. However, as metastable phases, they can exist at much higher pressures. Kyanite, the dense structure of which is based upon cubic closest packing of oxygen atoms, can persist as a metastable phase up to at least 80 GPa; the same is true for the hypothetical dense pseudobrookite-like and V_3O_5-like phases of Al_2SiO_5 (Oganov & Brodholt, 2000). Using *ab initio* simulations, we found that the low-density phases, andalusite and sillimanite, spontaneously undergo extremely interesting phase transitions in the region 35–55 GPa. These transitions are the subject of the present study.

2. Computational methodology

We employed two distinct computer simulation methods: (i) first-principles pseudopotential calculations and (ii) semi-classical calculations, based on empirically derived interatomic potentials. Quantum-mechanical calculations are very accurate and reliable, but computationally expensive. Their results comprise the main quantitative basis for our discussion of structural and thermodynamic aspects of the phase transitions. More approximate semi-classical calculations, which are very cheap in terms of CPU time (about 10^3 times faster than the first-principles calculations), can be used efficiently for dynamical as well as for static calculations. This technique is employed here for studying dynamical properties at a qualitative level.

Calculations of both types require approximate lattice parameters and atomic coordinates of each phase as input; the compression behaviour of each mineral is then studied separately. Theoretically, a structure can be metastable under given conditions if there are no net forces acting on the atoms at rest and there are no soft modes. As our calculations show, andalusite and sillimanite can persist as metastable phases up to *ca* 35–55 GPa; at these pressures, they cease to be in the local free-energy minima (soft modes appear) and spontaneously transform into other metastable phases.

2.1. First-principles calculations

First-principles calculations were performed using the *VASP* code (*Vienna Ab Initio Simulation Package*; Kresse & Furthmuller, 1996) running on the Cray T3E supercomputers at Edinburgh Parallel Computer Centre and Manchester Computer Centre. The computational method is based on density functional theory (Hohenberg & Kohn, 1964; Kohn & Sham, 1965) within the generalized gradient approximation (GGA) (Wang & Perdew, 1991).

Valence-orbital one-electron wavefunctions were expanded in a plane-wave basis set with a plane-wave kinetic energy cutoff of 800 eV (1 eV = 96.485 kJ mol^{-1}), which was found to give the total energy converged to within 6×10^{-4} eV atom^{-1}. The effects of the core electrons were modelled by effective core pseudopotentials (ECPs). All adopted pseudopotentials were non-local: norm-conserving (Rappe *et al.*, 1990) with partial core corrections (Louie *et al.*, 1982) for Al (valence configuration $3s^2 3p^1 3d^0$) and Si (valence configuration $3s^2 3p^2 3d^0$), and ultrasoft ECP (Vanderbilt, 1990) for O (valence configuration $2s^2 2p^4 3d^0$). Core-region cutoffs were 0.96 Å for Al, 0.95 Å for Si and 0.82 Å for O. It is important to note that all these ECPs were generated using the same density functional (Wang & Perdew, 1991) as used in our solid-state calculations; all these ECPs were taken from the *VASP* pseudopotential library. For the purpose of studying phase transitions, symmetry constraints were not imposed in any of the calculations presented here. For the Brillouin-zone integration, we used the scheme of Monkhorst & Pack (1976) with $2 \times 2 \times 2$ grids. Increasing the k-point mesh density from $2 \times 2 \times 2$ to $4 \times 4 \times 4$ did not lead to changes in the total energy exceeding 1.5×10^{-3} eV atom^{-1}. Constant-pressure enthalpy minimization was carried out iteratively until self-consistency to within 10^{-3} eV for ionic relaxation and 10^{-4} eV for electronic relaxation was achieved. Stresses on the unit cell and forces on the atoms, used for structure relaxation, were calculated from the self-consistent charge density using the Hellmann–Feynman theorem.

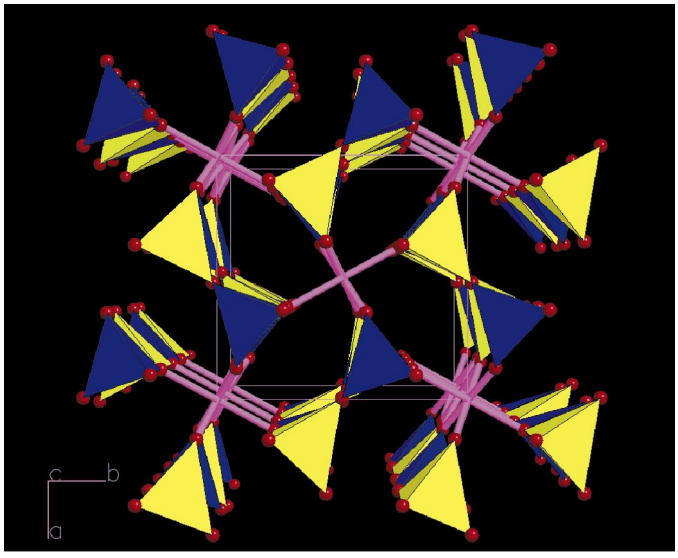

(*a*)

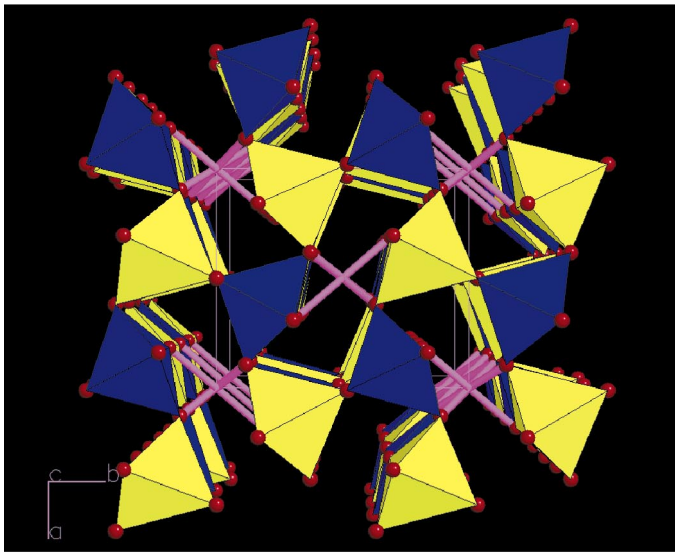

(*b*)

Figure 2
Crystal structures of (*a*) sillimanite and (*b*) meta-sillimanite phases. Si polyhedra are blue, Al2 polyhedra are yellow, Al1—O bonds are shown as purple sticks, and O atoms are red spheres. The unit-cell outline and orientation (in *Pbnm* setting) are also shown.

2.2. Semiclassical calculations

These calculations were performed with the *GULP* package (*General Utility Lattice Program*; Gale, 1997). Lattice dynamics is a key point in the theory of phase transitions. Unfortunately, non-empirical calculations are currently computationally too demanding to be used routinely for lattice dynamics, especially in the case of low-symmetry ionic crystals with large unit cells.

Here we use the simple ionic shell model, which proved to be sufficiently good to describe the lattice dynamics of silicate minerals (Burnham, 1990), including the Al_2SiO_5 polymorphs (Winkler & Buehrer, 1990; Rao *et al.*, 1999). The total lattice energy is given by

$$E_{st} = \sum_i k_s(\Delta r)^2 + \sum_{i \neq j}[z_i z_j / R_{ij} + b_{ij} \exp(-R_{ij}/\rho_{ij}) - c_{ij}/R_{ij}^6] + \sum_{i \neq j \neq k} k_{ijk}(\theta - \theta_0)^2, \quad (1)$$

where Δr denotes the distance between the core and shell of a polarizable ion, R_{ij} denotes an interatomic distance and θ is a valence angle. The first sum in (1) counts the self-energy of polarizable ions arising from their deformation, the second sum includes pair interactions (Coulombic energy plus short-range 6-exp Buckingham potential), while the third sum consists of three-body angle-bending terms. Coulombic energy was calculated by the Ewald summation; Buckingham potentials were summed over all interatomic pairs with distances below 10 Å; three-body potentials were calculated only between strong bonds (shorter than 1.8 Å for Si—O and 1.9 Å for Al—O bonds). Three-body terms are important for tetrahedrally coordinated silicates. For consistency, we use the same 'tetrahedral' three-body terms even for non-tetrahedral high-pressure structures, even though this can lead to some ambiguity. We use the same parameters as used by Urusov *et al.* (1998), which were taken from previous studies (Catlow, 1977; Sanders *et al.*, 1984; Lewis & Catlow, 1985) with a correction for the different coordination numbers of Al (see Lewis & Catlow, 1985; Urusov *et al.*, 1998).

Crystal structures were determined by minimizing the lattice enthalpy in the constant-pressure regime. Elastic constants were computed as the second derivatives of the lattice energy density with respect to lattice strains, and

Table 3
Crystal structure and equation of state of the meta-sillimanite phase.

	GULP (30 GPa)	*VASP* (50 GPa)
Unit-cell parameters and volume		
a_0 (Å)	5.891	6.178
b_0 (Å)	7.443	7.135
c_0 (Å)	6.044	5.773
V (Å^3)	265.00	254.49
Atomic coordinates (space group *Pbnm*)		
Al1	(0, 0, 0)	(0, 0, 0)
Al2	(0.1189, 0.3126, 1/4)	(0.1151, 0.3047, 1/4)
Si	(0.1215, 0.3064, 3/4)	(0.1249, 0.2915, 3/4)
O_a	(0.3939, 0.3755, 3/4)	(0.3829, 0.3721, 3/4)
O_b	(0.4002, 0.3793, 1/4)	(0.3892, 0.3747, 1/4)
O_c	(0.5089, −0.0139, 3/4)	(0.4987, −0.0167, 3/4)
O_d	(0.1605, 0.2079, 0.5071)	(0.1843, 0.1853, 0.5060)
$E(V)$ equation of state (*VASP* data)		
E_{atom} (eV)		−49.861
V_0 (Å^3)		325.68
K_0 (GPa)		112.50
K'		4.73

normal mode frequencies were derived from the eigenvalue equation (see Dove, 1993):

$$\det|\mathbf{D}^{ij}_{\alpha\beta}(\mathbf{q}) - \omega^2\delta_{\alpha\beta}\delta_{ij}| = 0, \quad (2)$$

where $\mathbf{D}$ is the dynamical matrix and ω^2 are its eigenvalues. Negative ω^2 (*i.e.* imaginary ω) signify dynamical instability of the structure with respect to a particular atomic motion, given by the mode eigenvectors, and indicate a soft-mode-driven phase transition. The soft-mode wavevector $\mathbf{q}$ determines the direction and periodicity of the modulation imposed on the parent lattice at the phase transition.

An important particular case of dynamical instability is mechanical instability, in which long-wavelength acoustic modes soften. The necessary and sufficient condition of mechanical stability of a crystal is positive definiteness of the elastic-constant tensor C_{ij} (Fedorov, 1968; Sirotin & Shaskolskaya, 1975). Positive definiteness is equivalent to positiveness of the determinant of the C_{ij} matrix and all its principal minors; in particular, all diagonal elements C_{ii} are principal minors and, therefore, must be positive for a mechanically stable crystal. Mechanical stability conditions for crystals of all symmetry classes have been analysed previously (Cowley, 1976; Terhune *et al.*, 1985). Violation of any of these conditions leads to softening of an acoustic mode in the vicinity of the Γ point, inducing a ferroelastic phase transition. Mechanical stability criteria for crystals under stress (Wang *et al.*, 1993, 1995) employ the C_{ij} derived from the stress–strain relations.[3]

2.3. Accuracy of simulations

Tables 1 and 2 present a comparison of the calculated and experimentally determined crystal structures and properties of andalusite and sillimanite at ambient pressure.[4] Equations of state were fitted to the third-order Birch–Murnaghan equation of state:

$$P(V) = 3/2K_0[(V_0/V)^{7/3} - (V_0/V)^{5/3}]\{1 + \xi[(V_0/V)^{2/3} - 1]\}, \quad (3)$$

where V_0 and K_0 are the zero-pressure volume and bulk modulus, respectively, and $\xi = 3/4(K_0' - 4)$, in which K_0' is the pressure derivative of the bulk modulus at $P = 0$. In terms of the internal energy as a function of volume, $E(V)$, this equation of state can be equivalently written as

$$\begin{aligned} E(V) = E(V_0) + 3/2K_0V_0[&3/2(\xi - 1)(V_0/V)^{2/3} \\ &+ 3/4(1 - 2\xi)(V_0/V)^{4/3} + 1/2\xi(V_0/V)^{6/3} \\ &- (2\xi - 3)/4]. \end{aligned} \quad (4)$$

As can be seen from Tables 1 and 2, both types of simulations reproduce experimental data fairly well. In the sense of

Table 4
Geometry (Å, °) of the SiO_5 polyhedra.

Results for meta-quartz are according to Badro *et al.* (1997), obtained in the local-density approximation at 16 GPa. The meta-quartz phase is a metastable phase that is isosymmetric with quartz and succeeds it at high non-hydrostatic pressures. The polyhedron described by Badro *et al.* (1997) is very similar to our results. In our polyhedron, the O4 and O5 vertices are symmetrically equivalent, but in the polyhedron of Badro *et al.* (1997) they are different. Two entries relate to the two symmetrically distinct parameters of the polyhedron of Badro *et al.* (1997).

	Meta-sillimanite (*GULP*, 30 GPa)	Meta-sillimanite (*VASP*, 50 GPa)	Meta-quartz (SiO_2)
Si—O1	1.685	1.695	1.728
Si—O2	1.901	1.878	1.869
Si—O3	1.543	1.567	1.617
Si—O4,5	1.657 (×2)	1.641 (×2)	1.674; 1.626
O1—Si—O2	151.1	160.7	168.2
O1—Si—O3	102.1	99.3	93.7
O1—Si—O4,5	90.2	86.9	95.9
O2—Si—O3	106.8	100.0	87.6
O2—Si—O4,5	76.9	83.2	76.3; 94.6
O3—Si—O4,5	116.9	120.8	142.4; 106.1
O4—Si—O5	124.7	118.3	108.9

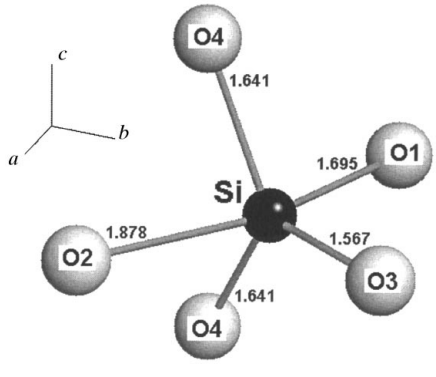

Figure 3
Geometry of the SiO_5 polyhedra in the meta-sillimanite structure (*VASP* results at 50 GPa). Crystallographic types of oxygen atoms and their distances to the Si atom are indicated. The inset shows the unit-cell orientation. This geometry can be described either as a trigonal bipyramid (with apical O4 atoms) or as a square pyramid (apical O3 atom). The orientation with respect to the unit-cell (*Pbnm*) axes is indicated.

[3] There is a simple correction (Barron & Klein, 1965; Wallace, 1972) to transform between the C_{ij} derived from the energy-density derivatives and those obtained from stress–strain relations.
[4] Tables of structural parameters at all pressures are available from the authors.

quality of results, *ab initio* GGA calculations are superior. The GGA calculations predict clearly better atomic fractional coordinates. As in almost all known cases, GGA calculations produce unit-cell parameters that are systematically overestimated by *ca* 1%, with a corresponding underestimation of the bulk modulus by *ca* 10% (Oganov *et al.*, 2001). Both methods give a reasonably good equation of state for each mineral. It is known that semi-classical calculations are unreliable in predicting phase-transformation enthalpies when large structural changes are involved, *e.g.* for transitions between kyanite, andalusite and sillimanite (Winkler *et al.*, 1991). Unlike the ionic model calculations, the *ab initio* calculations based on the GGA successfully reproduce the phase diagram (Fig. 1) of the Al_2SiO_5 system (Oganov & Brodholt, 2000). GGA calculations are also very successful in obtaining accurate atomization energies. However, both methods give a very similar qualitative picture of the metastable and largely structure-conserving pressure-induced phase transitions in andalusite and sillimanite. Only the transition pressures predicted by semiclassical calculations are ~2 times lower than the *ab initio* values. Although the GGA usually results in a shifted pressure scale (Oganov *et al.*, 2001) and overestimates the transition pressures (for a discussion, see Zupan *et al.*, 1998; Oganov & Brodholt, 2000), the errors are usually within a few GPa. In the following discussion, we use only the GGA pressures.

3. Phase transitions in sillimanite

The change in structure occurring upon compression above 33.5 GPa can be seen in Fig. 2. The low- and high-pressure phases have the same symmetry, *Pnma*, and similar structures; the Al1 positions are octahedrally coordinated in both structures. The difference is that, in the high-pressure meta-sillimanite phase, all Si atoms and half of the Al atoms (Al2 positions) display fivefold coordination instead of the tetrahedral coordination they adopt in sillimanite. This is achieved by pulling the O atoms, initially not bonded to Si and Al2, inside the first coordination spheres of Si and Al2. The increase in coordination numbers is, as usual, correlated with the increase in density upon the transition. Structural parameters of the meta-sillimanite phase are given in Table 3.

Five-coordinate Si was discovered in an inorganic compound ($K_2Si_4O_9$ glass) only recently (Stebbins & McMillan, 1989), using NMR spectroscopy; the first structural characterization of five-coordinate Si was obtained for $CaSi_2O_5$ (Angel *et al.*, 1996), almost simultaneously with a theoretical prediction of a metastable SiO_2 phase with five-

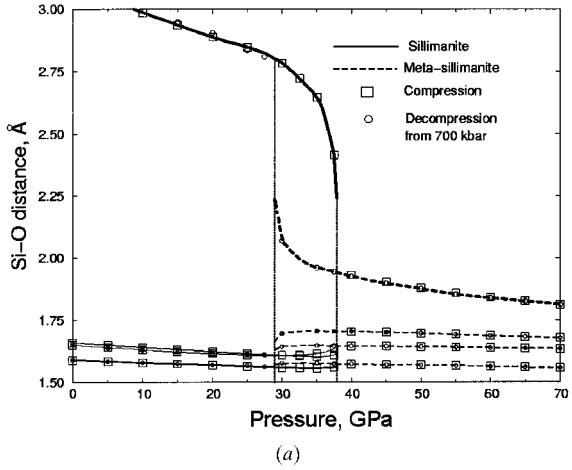

Figure 4
Evolution of (*a*) Si—O and (*b*) Al—O distances in sillimanite. Vertical lines show the hysteresis loop.

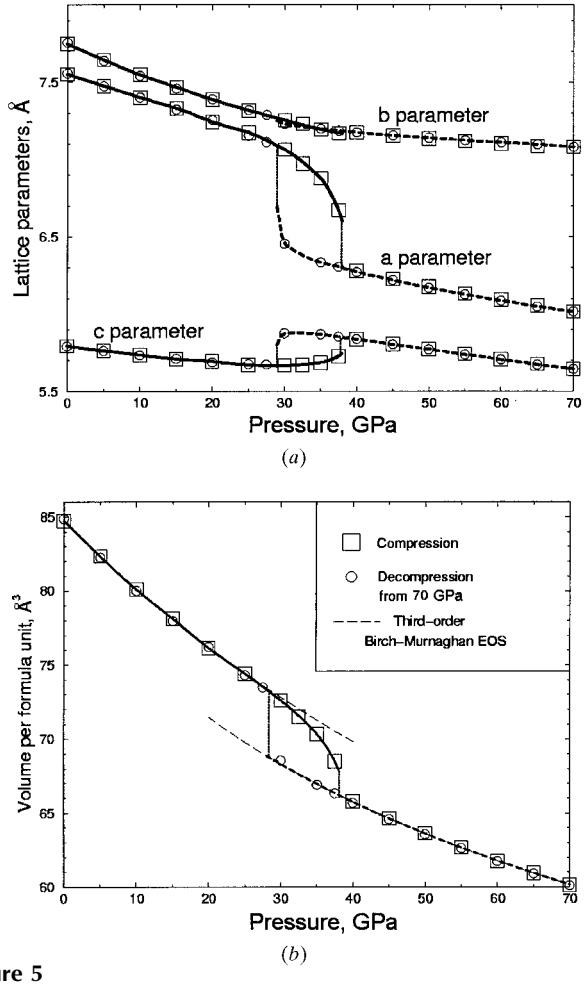

Figure 5
Pressure evolution of (*a*) the lattice parameters and (*b*) the unit-cell volume of sillimanite. The hysteresis loop is very pronounced.

coordinate Si atoms (Badro *et al.*, 1997). Using quantum-mechanical simulations, Warren *et al.* (1999) considered the pressure-induced transition between the phases of $CaSi_2O_5$ containing Si in octahedral and fivefold coordination. Another case of this exotic coordination of Si was found in a recent experimental study (Alberti *et al.*, 1999) of temperature-induced dehydration of the zeolite mineral brewsterite [$(Sr,Ba)Al_2Si_6O_{16}\cdot 5H_2O$]. Molecular dynamics simulations

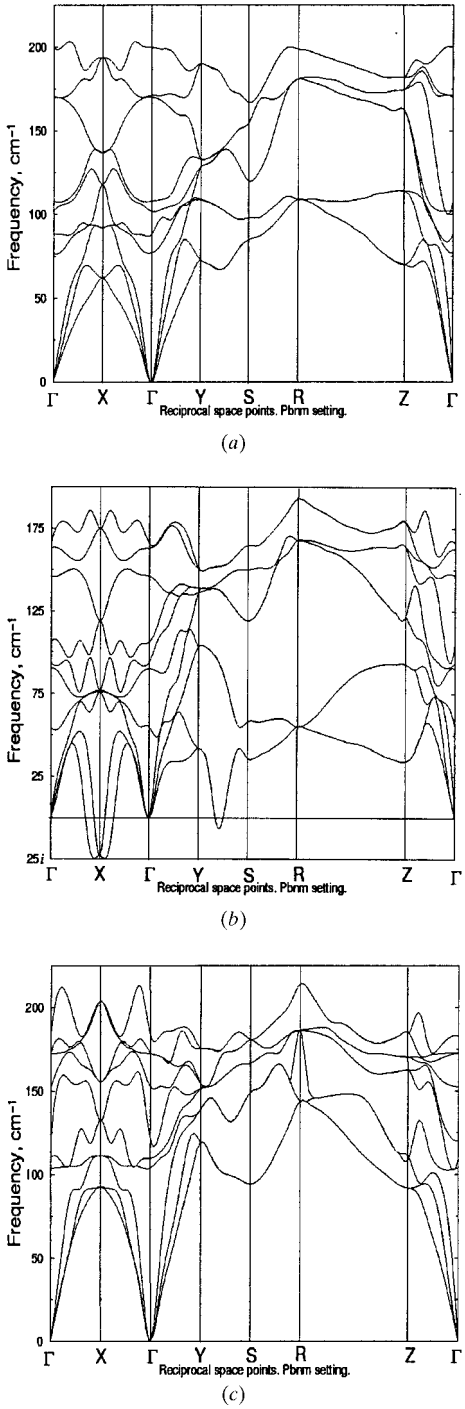

Figure 6
Phonon dispersion curves of (*a*) sillimanite at room pressure, (*b*) sillimanite near the transition to the isosymmetric phase, and (*c*) the isosymmetric phase. Only several lowest-frequency phonon branches are shown. *Pbnm* setting is used in the notation of reciprocal-space points.

(Chaplot & Choudhury, 2000) of $MgSiO_3$ enstatite have indicated a phase containing five-coordinate Si roughly at the pressure–temperature conditions of the Earth's transition zone. This phase is almost certainly metastable and appears as an intermediate step in the pressure-induced transformation from enstatite (Si in tetrahedral coordination) to $MgSiO_3$ perovskite (Si in octahedral coordination). Our work reports a further example of this unusual coordination. The interest in five-coordinate Si is mainly prompted by its anticipated importance for the transport properties in the Earth's mantle (see Angel *et al.*, 1996, and references therein), because the fivefold coordination, intermediate between tetrahedral and octahedral coordination, is likely to appear in fluids, especially at pressures corresponding to the change of the coordination number of Si in mantle minerals (8–30 GPa), and can serve as a convenient transition state in mass transport.

In Table 4 and Fig. 3, we analyse the geometry of the SiO_5 polyhedra determined by our calculations. Comparison with the other two studies (Angel *et al.*, 1996; Badro *et al.*, 1997) indicates similarities with the study of Badro *et al.* (1997), who also found one Si—O bond to be noticeably longer than the others, and the overall geometry of the polyhedron to be intermediate between a trigonal bipyramid and a square pyramid, rather than a square pyramid as found by Angel *et al.* (1996) in $CaSi_2O_5$. The difference is easy to explain by the genesis of these polyhedra. In the low-pressure titanite-like $CaSi_2O_5$ studied by Angel *et al.* (1996), the SiO_5 polyhedra were formed by removing one O atom from SiO_6 octahedra of the high-pressure phase, naturally producing a square pyramid. In SiO_2 (Badro *et al.*, 1997) and Al_2SiO_5 (this work), SiO_5 polyhedra are formed by adding one O atom to SiO_4 tetrahedra, which results in a trigonal bipyramid. The two types of polyhedra, however, can be converted to each other by small displacements of O atoms; this transformation is known as the Berry pseudorotation.

In Fig. 4, one can see how Al—O and Si—O distances evolve with pressure: when an initially non-bonding 'fifth' Al···O or Si···O contact reaches some threshold distance, a bond is formed. The bond formation changes the topology of the crystal structure and the force balance within it, making it collapse into the higher-density phase. On decompression, the exactly opposite situation occurs: when a bond becomes too long, it ceases to be a bond and the non-bonded atom is expelled from the coordination sphere. In other words, the formation of the new bond or destruction of an old one is the cause of the phase transition. The critical interatomic distances, which we find to be *ca* 2.25 (17) and 2.05 (4) Å for Si—O and Al—O bonds, respectively, can be used as a criterion of bonding in oxygen compounds of Al and Si, and are potentially important in studies of the structure of glasses and transition states in these systems. It is interesting that purely ionic shell model calculations reproduce these critical lengths remarkably well: 2.27 (15) Å for Si—O and 2.01 (2) Å for Al—O bonds. Therefore, the nature of the critical bonding distances in Al_2SiO_5 is not related to the changes in electronic structure, which are not accounted for by the simple ionic shell model. Bond valences, calculated using the parameters of

Brown & Altermatt (1985), are 0.18 and 0.34 valence units, respectively (for the ionic model, 0.17 and 0.34, respectively). The Al—O critical bond length [2.05 (4) Å] seems to be too small; a better value (~2.4 Å) would result if we take the structure before the onset of the incommensurate modulation (see below) occurring in sillimanite in the region of the anomalous softening of the structure in the hysteresis region. It is possible that this incommensurate modulation and softening reflect the steric strain associated with the formation of the new Al—O bonds.

The pressure-induced variation of the unit-cell parameters and volume is shown in Fig. 5. Several features deserve special note. This phase transition, with an equilibrium transition pressure of 33.5 GPa, is reversible; in Fig. 5 we show results obtained on decompression as well as on compression. The transition is first order with a marked volume discontinuity and strong hysteresis (which is a necessary feature of all reversible first-order transitions). This agrees with the conclusion of Bruce & Cowley (1981) and Christy (1995), who have shown, on the basis of Landau theory, that isosymmetric phase transitions must be of first order, but can disappear (*i.e.* become fully continuous) at temperatures above the critical point. The lattice parameters and volume display normal pressure dependence outside the hysteresis region. Inside that region, we observe an anomalously large fall of the volume and parameter *a* with increasing pressure, and non-monotonic variation of the parameter *c*, which increases with pressure near the transition. Parameter *b* is affected only slightly by the phase transformation. The negative linear compressibility along the *c* axis, which we have found in sillimanite and its high-pressure isosymmetric successor in the transition region, is a very interesting phenomenon. Bulk compressibility cannot be negative, as this is forbidden by mechanical stability criteria. Linear compressibility, however, can be negative in some directions for non-cubic crystals. In our case, it was associated with an incipient phase transition and formation/breaking of new bonds in the structure.[5] This isosymmetric transition is ferroelastic because it is associated (as shown by *GULP* calculations) with a complete softening of the C_{11} elastic constant. This correlates with the collapse of the *a* axis, associated with the formation of new Si—O and Al—O bonds directed largely along the *a* direction.

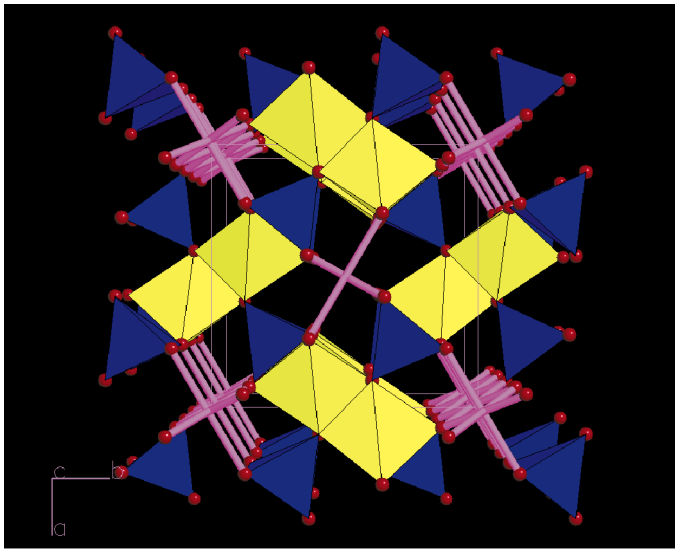

(*a*)

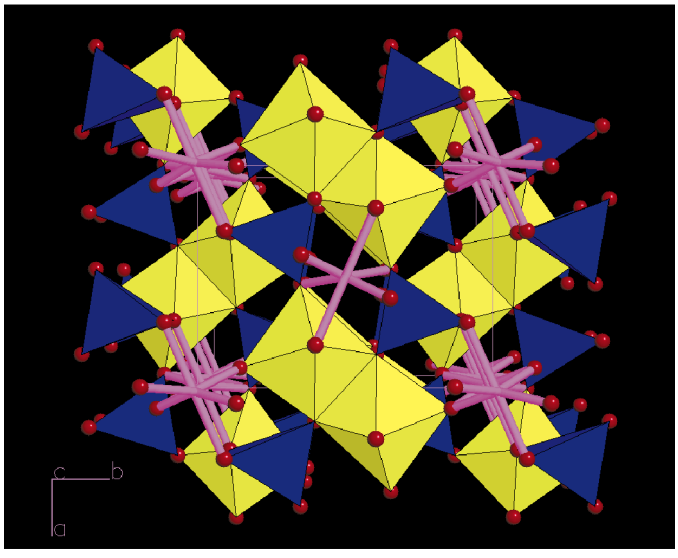

(*b*)

Figure 7
Crystal structures of (*a*) andalusite and (*b*) the high-pressure isosymmetric dynamically unstable phase. Instead of the latter phase, an amorphous solid is predicted to occur at high pressures. Si polyhedra are blue, Al2 polyhedra are yellow, Al1—O bonds are shown as purple sticks, and O atoms are red spheres. The unit-cell outline and orientation are also shown.

Variation of the lattice parameters in the vicinity of the transition suggests that structures of both phases 'prepare' for the transition, *i.e.* their lattice parameters tend to merge towards the transition. It is well known (Sirotin & Shaskolskaya, 1975) that, for structural transitions with symmetry breaking, the structure of the low-symmetry phase becomes increasingly more similar to the high-symmetry structure, whereas the latter shows no indication of approaching the low-symmetry structure. As our example suggests, in cases where the symmetries of the phases are identical, both structures show a tendency to approach each other in the vicinity of the transition.

Using semi-classical simulations, we considered dynamical stability criteria (Fig. 6). At ambient pressure, sillimanite is dynamically stable, in agreement with experiment. The high-pressure isosymmetric phase is also dynamically stable. However, at *ca* 1 GPa below the high-pressure transition, sillimanite acquires a minor dynamical instability, which would lead to an incommensurate modulation with $\mathbf{q}^* \simeq (0.47, 0, 0)$ (Fig. 6*b*). The imaginary frequencies are very small, suggesting that the modulation may be anharmonically suppressed, even at not very high temperatures, and the isosymmetric phase transition would occur, bypassing the incommensurate phase.

[5] In $Pb_3(PO_4)_2$, negative linear compressibility was found along the *c* direction of the monoclinic cell (Angel, 2000); it was tentatively ascribed to the stereochemical activity of the lone electron pair of Pb^{2+} (Angel, private communication).

Several 'spot-checks' were performed using both *VASP* and *GULP* in order to make sure that the input structure did not bias the results. These spot-checks started with a slightly deformed unit cell (by 0.01–0.02 Å and 1–2°) and with displaced atoms (by 0.01–0.02 Å), picked at random, followed by static constant-pressure relaxation of the structure. For the high-pressure sillimanite modification, the original structure was always recovered in *VASP* calculations, even at pressures as high as 70 GPa. At the same time, at ∼10 GPa after the formation of the isosymmetric phase, *GULP* calculations show soft modes and difficulties in optimizing the structure and removing the introduced strains; however, this results from the inadequacy of the three-body potentials, which becomes critical at these high pressures as all five Si—O (and Al—O) bonds become strong (*i.e.* shorter than 1.8 and 1.9 Å for Si—O and Al—O bonds, respectively).

4. Phase transitions in andalusite

Andalusite appears to be metastable in a much broader pressure range, up to 52 GPa. The crystal structures of andalusite and the meta-andalusite phase succeeding it are depicted in Fig. 7. The equations of state and pressure evolution of the lattice parameters are represented in Fig. 8, which shows an extremely large hysteresis region, in the range 17–52 GPa. The meta-andalusite phase, however, is dynamically unstable at all pressures. The character of the dynamical instability (Fig. 9), involving softening of almost a whole transverse acoustic branch along some directions, suggests amorphization of this structure (Binggeli *et al.*, 1994; Keskar *et al.*, 1994), the appearance of which is therefore nothing more than an artifact of periodic boundary conditions. In this unstable phase, all Al atoms are octahedrally coordinated, while in andalusite the Al2 positions are five-coordinate, and the Si atoms have tetrahedral coordination. In order to make sure that amorphization does occur, we performed several static spot-checks using the method described in the previous section. The fact that the structure of the high-pressure successor of andalusite was not recovered is clear evidence of its instability. The resulting structure drastically differs from the original structure in the unit-cell volume and shape. *GULP* calculations still find some soft modes for this structure,

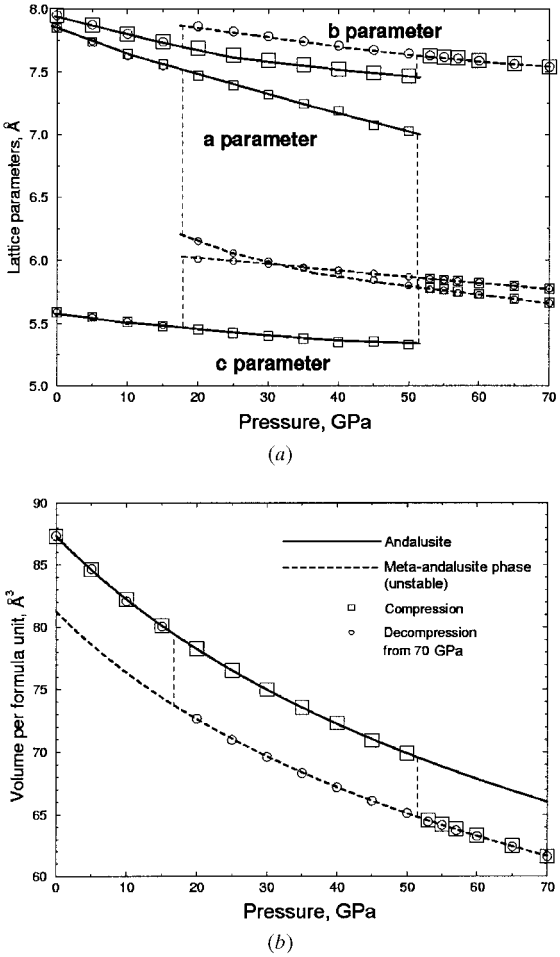

Figure 8
Pressure evolution of (*a*) the lattice parameters and (*b*) the unit-cell volume of andalusite. Dashed lines show the hysteresis loop.

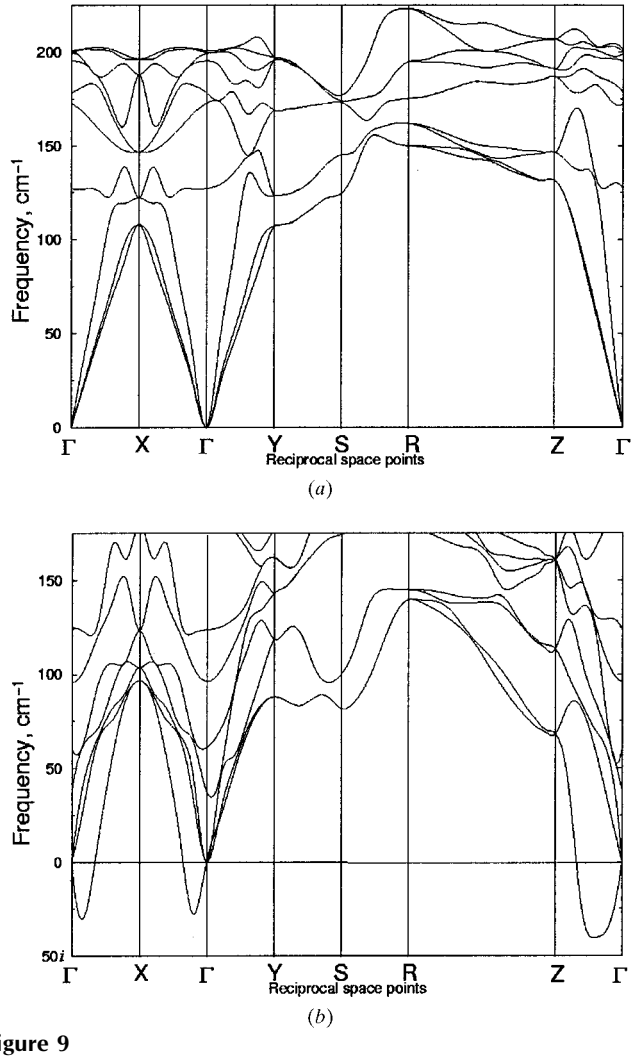

Figure 9
Phonon dispersion curves of (*a*) andalusite at room pressure and (*b*) the high-pressure post-andalusite phase, showing its dynamical instability. Only several lowest-frequency phonon branches are shown. Amorphization should occur along the *c* and, possibly, *a* axes.

suggesting that larger supercells are necessary to describe the relaxation of this amorphous structure correctly.

The pressure evolution of the lattice parameters (Fig. 8) and interatomic distances indicates no 'preparation' for the transition of the kind we encountered in sillimanite. Instead, the transition is abrupt, apparently being caused by cooperative rather than local effects driving the crystal to dynamical instability. Although the crystal structures of andalusite and sillimanite are quite similar, the drastic difference between their high-pressure behaviour arises from the difference in the degree of flexibility of the structural units, which are rather supple in sillimanite and rigid in andalusite. Consequently, andalusite can stay metastable up to much higher pressures than sillimanite and the transformation is not associated with the critical bond mechanism discussed in the previous section.

5. Discussion and conclusions

Using *ab initio* simulations, we have predicted here a number of metastable modifications of Al_2SiO_5. Sillimanite undergoes an isosymmetric phase transition at 33.5–38 GPa, preceded by an incommensurate transition at low temperatures. Andalusite transforms directly into an amorphous phase at 34–51 GPa. We have analysed the geometry of the SiO_5 polyhedra found in the high-pressure meta-sillimanite phase. These polyhedra can be described as intermediate between trigonal bipyramids and square pyramids, just as those studied by Badro *et al.* (1997) in a metastable isosymmetric phase formed from quartz (SiO_2). A trigonal bipyramid is likely to be formed by the addition of an O atom to an SiO_4 tetrahedron on increasing pressure, while, for a square pyramid, the case of removal of one O atom from an SiO_6 octahedron on decreasing pressure is more relevant (Fig. 10). Apart from direct results on the given system, this study provides several general conclusions.

First, we have proposed the existence of a critical bonding distance R_{CR}, and transferability of the R_{CR} values between different crystals. This concept naturally explains the metastable phase transitions in sillimanite and should be able to explain a number of other displacive phase transitions. With the R_{CR} value known, it becomes easy to determine unambiguously the coordination numbers of atoms, which is often difficult, *e.g.* for ionic crystals with large cations. Therefore, the R_{CR} criterion, if robust enough, should bring more order into the structural chemistry of such compounds. The fact that the R_{CR} values determined by quantum-mechanical calculations and simple interatomic potentials are identical implies that R_{CR} is not sensitive to the details of electronic structure and its changes.

Second, we can generally expect that, for crystals with complicated low-symmetry structures and many degrees of freedom, metastable pressure-induced phase transitions should be very common. In such systems, the relaxation of internal degrees of freedom under pressure would easily lead to situations where initially non-bonded atoms approach each other closely enough ($R < R_{CR}$) to form a new bond, which automatically triggers a phase transition. Systems potentially of this kind, namely titanite-like $CaSi_2O_5$, quartz and coesite (SiO_2), feldspars, zeolites and berlinite ($AlPO_4$), all undergo such transitions. As structures tend to accommodate the minimum changes necessary to maintain stability, symmetry will be preserved whenever possible. We call such transitions 'local' (the old and new phases are structurally related and the new phase may be metastable) as opposed to 'global' (where there are no structural relations between the old and new phases and the new phase is always thermodynamically stable, *i.e.* it is in the global free-energy minimum). The idea of local and global transitions is very powerful, taking its strength from a simple link it establishes between structure, thermodynamics and kinetics. For example, the Ostwald rule takes a simple form: 'global phase transformations tend to occur *via* a

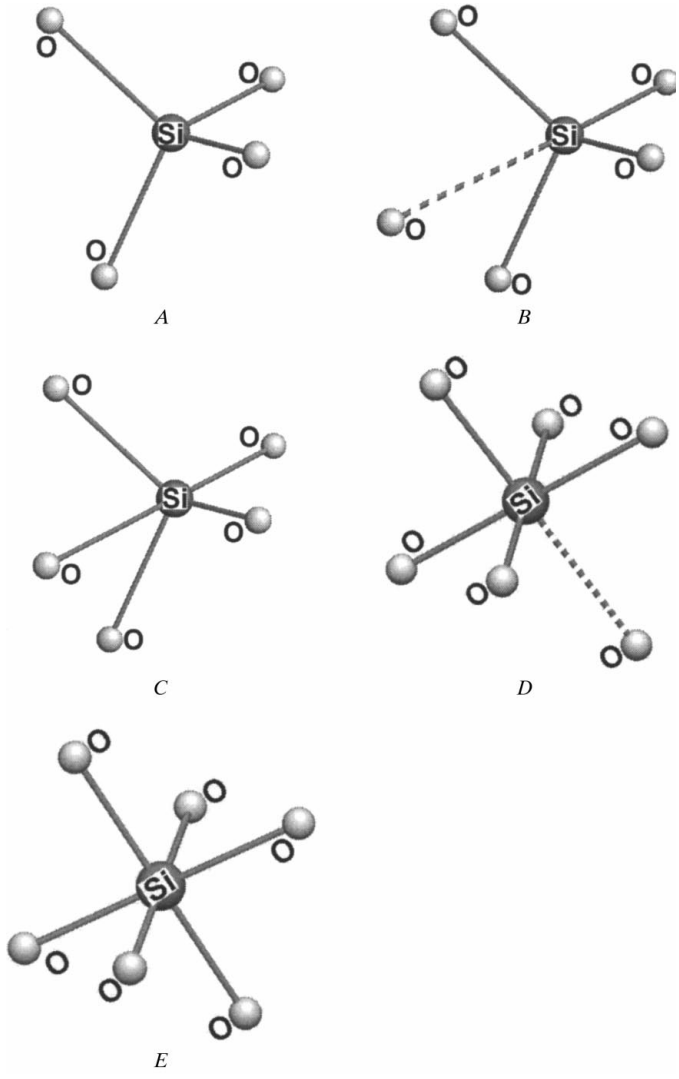

Figure 10
Genesis of the fivefold coordination of silicon. Tetrahedral Si (*A*) can capture a neighbouring O atom (*B*), becoming fivefold coordinated (*C*). The coordination polyhedron is intermediate between a trigonal bipyramid and a square pyramid (*cf.* Fig. 3), into which it can easily transform by Berry pseudorotation ($C \rightarrow D$). Capturing another O atom, a square bipyramid becomes an octahedron ($D \rightarrow E$). The reverse transformation path is equally possible. In this study, we see stages *A*–*C*; Angel *et al.* (1996) and Warren *et al.* (1999) observed stages *D*–*E* in $CaSi_2O_5$.

sequence of local transitions'. From this viewpoint, it is easy to conclude that the phases that are most likely to appear as metastable in synthesis must either have a stability domain on the pressure–temperature phase diagram or be related to one of such phases by a local phase transition. This implies structural and symmetry relations between the possible metastable phases and the stable phases for a system. These and related ideas will be explored in a following paper.

ARO is grateful to Paul McMillan, Ross Angel and Tonci Balič-Zunič for useful discussions, and Georg Kresse for permission to use the *VASP* code in this work. Funding of the research by ARO at UCL through the Russian President Scholarship for Education Abroad, the UCL Graduate School Research Scholarship and the UK Overseas Research Scholarship is acknowledged. CPU time allocation on the CRAY T3E supercomputers was provided by the British NERC.

References

Alan, D. R. & Nelmes, R. J. (1996). *J. Phys. Cond. Matter*, **8**, 2337–2363.
Alberti, A., Sacerdoti, M., Quartieri, S. & Vezzalini, G. (1999). *Phys. Chem. Miner.* **26**, 181–186.
Angel, R. J. (2000). *Reviews in Mineralogy and Geochemistry*, Vol. 39, *Transformation Processes in Minerals*, edited by S. A. T. Redfern & M. A. Carpenter, pp. 85–104. Washington, DC: Mineralogical Society of America.
Angel, R. J., Ross, N. L., Seifert, F. & Fliervoet, T. F. (1996). *Nature (London)*, **384**, 441–444.
Badro, J., Teter, D. M., Downs, R. T., Gillet, P., Hemley, R. & Barrat, J.-L. (1997). *Phys. Rev. B*, **56**, 5797–5806.
Barron, T. H. K. & Klein, M. L. (1965). *Proc. Phys. Soc.* **85**, 523–532.
Binggeli, N., Keskar, N. R. & Chelikowsky, J. R. (1994). *Phys. Rev. B*, **49**, 3075–3081.
Brown, I. D. & Altermatt, D. (1985). *Acta Cryst.* B**41**, 244–247.
Bruce, A. D. & Cowley, R. A. (1981). *Structural Phase Transitions*. London: Francis and Taylor.
Burnham, C. W. (1990). *Am. Mineral.* **75**, 443–463.
Catlow, C. R. A. (1977). *Proc. R. Soc. London Ser. A*, **353**, 533–561.
Chaplot, S. L. & Choudhury, N. (2000). *Solid State Commun.* **116**, 599–603.
Christy, A. G. (1995). *Acta Cryst.* B**51**, 753–757.
Cowley, R. A. (1976). *Phys. Rev. B*, **13**, 4877–4885.
Dove, M. T. (1993). *Introduction to Lattice Dynamics*. Cambridge University Press.
Fedorov, F. I. (1968). *Theory of Elastic Waves in Crystals.* New York: Plenum Press.
Gale, J. D. (1997). *J. Chem. Soc. Faraday Trans.* **93**, 629–637.
Hohenberg, P. & Kohn, W. (1964). *Phys. Rev.* **136**, B864–B871.
Iglesias, M., Schwarz, K., Blaha, P. & Baldomir, D. (2001). *Phys. Chem. Miner.* **28**, 67–75.
Kerrick, D. M. (1990). *Reviews in Mineralogy*, Vol. 22. *The Al_2SiO_5 Polymorphs*, pp. 37–110. Washington DC: Mineralogical Society of America.
Keskar, N. R., Chelikowsky, J. R. & Wentzcovitch, R. M. (1994). *Phys. Rev. B*, **50**, 9072–9078.
Kohn, W. & Sham, L. J. (1965). *Phys. Rev.* **140**, A1133–A1138.
Kresse, G. & Furthmuller, J. (1996). *Comput. Mater. Sci.* **6**, 15–50.
Kruger, M. B. & Jeanloz, R. (1990). *Science*, **249**, 647–649.
Lewis, G. V. & Catlow, C. R. A. (1985). *J. Phys. C*, **18**, 1149–1161.
Louie, S. G., Froyen, S. & Cohen, M. L. (1982). *Phys. Rev. B*, **26**, 1738–1742.
Mishima, O., Calvert, L. D. & Whalley, E. (1984). *Nature (London)*, **310**, 393–394.
Monkhorst, H. J. & Pack, J. D. (1976). *Phys. Rev. B*, **13**, 5188–5192.
Oganov, A. R. & Brodholt, J. P. (2000). *Phys. Chem. Miner.* **27**, 430–439.
Oganov, A. R., Brodholt, J. P. & Price, G. D. (2001). *Earth Planet. Sci. Lett.* **184**, 555–560.
Olbricht, W., Chatterjee, N. D. & Miller, K. (1994). *Phys. Chem. Miner.* **21**, 36–49.
Ralph, R. L., Finger, L. W., Hazen, R. M. & Ghose, S. (1984). *Am. Mineral.* **69**, 513–519.
Rao, M. N., Chaplot, S. L., Choudhury, N., Rao, K. R., Azuah, R. T., Montfrooij, W. T. & Bennington, S. M. (1999). *Phys. Rev. B*, **60**, 12061–12068.
Rappe, A. M., Rabe, K. M., Kaxiras, E. & Joannopoulos, J. D. (1990). *Phys. Rev. B*, **41**, 1227–1230.
Sanders, M. J., Leslie, M. & Catlow, C. R. A. (1984). *J. Chem. Soc. Chem. Commun.* **19**, 1271–1273.
Schmidt, M. W., Poli, S., Comodi, P. & Zanazzi, P. F. (1997). *Am. Mineral.* **82**, 460–466.
Sirotin, Yu. I. & Shaskolskaya, M. P. (1975). *Fundamentals of Crystal Physics.* Moscow: Nauka. (In Russian.)
Stebbins, J. F. & McMillan, P. F. (1989). *Am. Mineral.* **74**, 965–968.
Terhune, R. W., Kushida, T. & Ford, G. W. (1985). *Phys. Rev. B*, **32**, 8416–8419.
Tse, J. S. & Klug, D. D. (1992). *Science*, **255**, 1559–1561.
Urusov, V. S., Oganov, A. R. & Eremin, N. N. (1998). *Geokhimiya*, No. 5, pp. 456–474. (In Russian.) Engl. transl: *Geochem. Int.* **36**, 397–414.
Vanderbilt, D. (1990). *Phys. Rev. B*, **41**, 7892–7895.
Wallace, D. C. (1972). *Thermodynamics of Crystals*. New York: John Wiley.
Wang, Y., Li, J., Yip, S., Phillpot, S. & Wolf, D. (1995). *Phys. Rev. B*, **52**, 12627–12635.
Wang, Y. & Perdew, J. P. (1991). *Phys. Rev. B*, **44**, 13298–13307.
Wang, Y., Yip, S., Phillpot, S. & Wolf, D. (1993). *Phys. Rev. Lett.* **71**, 4182–4185.
Warren, M. C., Redfern, S. A. T. & Angel, R. J. (1999). *Phys. Rev. B*, **59**, 9149–9154.
Winkler, B. & Buehrer, W. (1990). *Phys. Chem. Miner.* **17**, 453–461.
Winkler, B., Dove, M. T. & Leslie, M. (1991). *Am. Mineral.* **76**, 313–331.
Winter, J. K. & Ghose, S. (1979). *Am. Mineral.* **64**, 573–586.
Yang, H., Hazen, R. M., Finger, L. W., Prewitt, C. T. & Downs, R. T. (1997). *Phys. Chem. Miner.* **25**, 39–47.
Zupan, A., Blaha, P., Schwarz, K. & Perdew, J. P. (1998). *Phys. Rev. B*, **58**, 11266–11272.